



*Dedicated to the memory of  
Professor Dumitru OANCEA (1941–2020)*

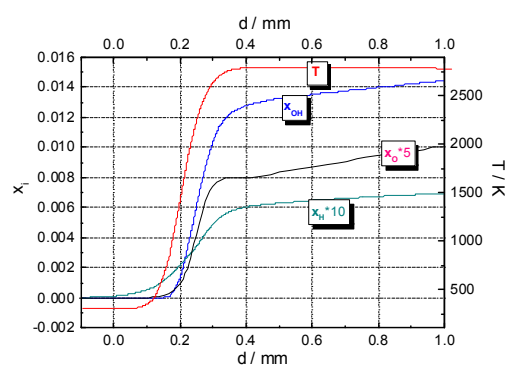
## LAMINAR FLAME PROPAGATION IN NITROGEN-DILUTED STOICHIOMETRIC H<sub>2</sub>-N<sub>2</sub>O MIXTURES – A NUMERICAL STUDY

Domnina RAZUS,\* Maria MITU, Venera GIURCAN and Codina MOVILEANU

“Ilie Murgulescu” Institute of Physical Chemistry, 202 Spl. Independenței, 060021 Bucharest, Roumania

Received September 30, 2020

The paper reports results of the detailed chemical modelling of isobaric deflagrations in stoichiometric H<sub>2</sub>-N<sub>2</sub>O-N<sub>2</sub> mixtures (N<sub>2</sub> = 20–60 vol%) at various initial temperatures (300–500 K) and various initial pressures (1–10 bar): laminar burning velocities, and profiles of temperature, volumetric heat release rate and species concentrations across the flame front. The dependence of the laminar burning velocity on temperature and pressure is examined by empirical power laws, for restricted ranges of pressure (or temperature) variation. For each examined composition, the laminar burning velocity correlates well with the volumetric rate of heat release and with the sum of mass fractions of reactive species in the flame front.



### INTRODUCTION

Besides its use as oxidant or nitriding agent in various industrial processes such as semiconductor manufacture or production of adipic acid and caprolactam,<sup>1,2</sup> nitrous oxide is increasingly used as additive that increases the power output of engines or as oxidizer replacing oxygen in propulsion systems of rockets, due to its large heat of formation (+81.6 kJ mol<sup>-1</sup>).<sup>3</sup>

Many data on flammability of gaseous fuel-nitrous oxide mixtures are currently reported, concerning mostly safety aspects of N<sub>2</sub>O handling: flammability limits,<sup>4-8</sup> minimum ignition energies,<sup>5,9</sup> explosion pressures and severity factors.<sup>10-13</sup> Among them, the H<sub>2</sub>-N<sub>2</sub>O mixture raises important safety issues, since it can easily

develop DDT (deflagration-to-detonation transition) especially at pressures and/or temperatures above ambient.<sup>14,15</sup> For safety reasons, the flammability limits of H<sub>2</sub>-N<sub>2</sub>O mixture and the stability of H<sub>2</sub>-N<sub>2</sub>O flames were determined at 70 mm Hg.<sup>16</sup> At ambient initial pressure, mixtures of H<sub>2</sub>-N<sub>2</sub>O with some amounts of N<sub>2</sub> and NH<sub>3</sub>, detected as emanation of nuclear wastes, were characterized by their flammability limits, ignition energies, flame speeds and laminar flame velocities.<sup>5</sup>

Among the parameters describing the flame propagation in premixed H<sub>2</sub>-N<sub>2</sub>O and H<sub>2</sub>-N<sub>2</sub>O-inert systems, the laminar burning velocity was most frequently reported<sup>16-27</sup> and it was constantly used to test the mechanisms developed for N<sub>2</sub>O conversion to other nitrogen-containing species,

\* Corresponding author: [drazus@icf.ro](mailto:drazus@icf.ro); [drazus@yahoo.com](mailto:drazus@yahoo.com). Tel: +40-21-3121147

and to update the rate coefficients of some elementary reactions of these compounds. Many studies on  $\text{H}_2/\text{N}_2\text{O}$  and  $\text{H}_2/\text{N}_2\text{O}/\text{NO}_2$  flames were focused on their structure, since these chemical systems are important for understanding NOx pollutant formation and reduction.<sup>21,22,25-30</sup>

The laminar flame propagation was studied in various conditions: as conical flames stabilized on a Bunsen burner,<sup>16,19</sup> as flat flames,<sup>17,23,28</sup> or as outwardly propagating flames in closed vessels.<sup>18,20,23-27</sup> Flame structure studies were made mostly with flames stabilized at sub-atmospheric pressures (20-70 mm Hg), characterized by a convenient front width, able to afford measurements of active species concentrations and of temperature profiles.<sup>18,20-22,28</sup> Most studies examined flames of inert-diluted  $\text{H}_2\text{-N}_2\text{O}$  mixtures with variable equivalence ratios, under variable inert concentrations at near-atmospheric initial conditions.<sup>19,20,23-25,27,28</sup> Some data on temperature and pressure influence on flame propagation in  $\text{H}_2\text{-N}_2\text{O}$  and  $\text{H}_2\text{-N}_2\text{O}$ -inert mixtures are known,<sup>16,19,27</sup> but only for restricted ranges of initial temperature and pressure variation. The modeling studies examined these experimental results,<sup>21-24,26,28,29</sup> with the scope to test and improve various detailed mechanisms describing oxidations supported by  $\text{N}_2\text{O}$ .

In the present study the influence of temperature and pressure on flame propagation in  $\text{H}_2\text{-N}_2\text{O}$  and  $\text{N}_2$ -diluted  $\text{H}_2\text{-N}_2\text{O}$  mixtures is examined by the computed laminar burning velocities, obtained using the detailed kinetic modeling of their flames. The stoichiometric composition of  $\text{H}_2\text{-N}_2\text{O}$  mixture (1:1 mole ratio) was chosen since it affords the system to reach the maximum value of its burning velocity.<sup>31</sup> The stoichiometric  $\text{H}_2\text{-N}_2\text{O}$  mixture, diluted with  $\text{N}_2$  (concentrations between 20 and 60 vol%) is examined at various initial temperatures between 300 and 500 K and various initial pressures between 1 and 10 bar. For each system, a correlation is sought between the burning velocity and the peak mass fractions of important radical species (H, HO and O) and with the peak rate of volumetric heat release in the flame. Sensitivity analyses in respect to laminar burning velocity are used to outline the reactions most influenced by pressure (and/or temperature) variation, with impact on reactive species concentrations.

## COMPUTING PROGRAMS

The kinetic modelling of  $\text{H}_2\text{-N}_2\text{O-N}_2$  flames was performed with 1D COSILAB package

developed by Rogg and Peters.<sup>32</sup> Premixed adiabatic laminar free flames were examined, using the GRI mechanism (version 3.0), based on 53 chemical species which participate to 325 elementary reactions. The mechanism was selected since it contains a comprehensive number of reactions involving N-containing species. Among the 53 species of GRI 3.0 mechanism, many were molecular or radical species containing C atoms. For them, low input mole fractions ( $1\text{E-}08$ ) were used; in this way the presence of C-containing species did not influence the output results of modeling. The runs were made for the isobaric combustion of  $\text{H}_2\text{-N}_2\text{O-N}_2$  at various pressures within 1 and 10 bar, various initial temperatures within 300 and 500 K and various mole fractions of  $\text{N}_2$ , and delivered the laminar burning velocities of gaseous mixtures, along with the temperature, volumetric rate of heat release and species profiles across the flame front.

As solvers, the package used a steady Newton solver (usually 25 iterations, relative tolerance  $10^{-5}$ ; absolute tolerance  $10^{-8}$ ), an unsteady Newton solver (usually 15 iterations, relative tolerance  $10^{-4}$ ; absolute tolerance  $10^{-6}$ ) and an unsteady Euler solver. The adaptive grid parameters were: GRAD = 0.1, CURV = 0.2, the maximum ratio of adjacent cell size between 1.3 and 1.1.

The input data were taken from thermodynamic and molecular databases of Sandia National Laboratories, USA, according to the international standard (format for CHEMKIN).

## RESULTS AND DISCUSSION

The initial temperature influence on laminar burning velocity for  $\text{H}_2\text{-N}_2\text{O}$  mixtures diluted with various nitrogen amounts is shown in Fig. 1, at initial pressures of 1 and 5 bar, respectively. Similar plots were drawn for all initial pressures and show the increase of laminar burning velocities with temperature. The data were analyzed using the empirical power law:

$$S_u = S_{u,ref} \left( \frac{T}{T_{ref}} \right)^\mu \quad (1)$$

where  $S_{u,ref}$  is the laminar burning velocity at reference temperature  $T_{ref}$ , and  $\mu$  is the thermal coefficient of laminar burning velocities. The thermal coefficients were calculated by a non-

linear regression analysis of  $S_u = f(T)$  at various initial pressures, choosing the ambient temperature as reference,  $T_{ref} = 298$  K. The results are given in Table 1. Initial pressure variation between 1 and 10 bar influence only slightly the thermal coefficients, which appear to depend only on the composition of flammable mixtures. They increase steadily as the nitrogen concentration grows larger and reach eventually (at  $N_2 = 60$  vol%) the usual range of values (1.60....1.70) reported for hydrocarbon-air mixtures.<sup>34,35</sup>

The initial pressure influence on laminar burning velocity, for  $H_2-N_2O$  mixtures diluted with various nitrogen amounts is shown in Fig. 2, at ambient initial temperature. Similar plots, drawn for  $H_2-N_2O$  mixture and  $H_2-N_2O-N_2$  mixtures at different initial temperatures, are given in Fig. 3(a) and (b). The data show the decrease of laminar burning velocities at pressure increase. At constant

initial temperature, the laminar burning velocities variation against pressure was analyzed with the power law equation:

$$S_u = S_{u,ref} \left( \frac{p}{p_{ref}} \right)^\nu \quad (2)$$

where  $\nu$  is the baric coefficient and  $S_{u,ref}$  is the laminar burning velocity at reference pressure  $p_{ref}$ , usually chosen as the ambient pressure.

The baric coefficients  $\nu$ , calculated by a non-linear regression analysis of  $S_u = f(p)$  within the pressure range 1–10 bar, at various initial temperatures and various nitrogen concentrations, are given in Table 2.

Table 1

Thermal coefficients,  $\mu$ , of laminar burning velocities for the stoichiometric  $H_2-N_2O$  mixture diluted with various  $N_2$  amounts, at various initial pressures

$N_2$ /vol% $p_0$ / bar	0	20	40	60
1	$1.33 \pm 0.02$	$1.42 \pm 0.02$	$1.42 \pm 0.02$	$1.58 \pm 0.03$
3	$1.34 \pm 0.02$	$1.46 \pm 0.04$	$1.44 \pm 0.04$	$1.62 \pm 0.05$
5	$1.35 \pm 0.02$	$1.45 \pm 0.02$	$1.45 \pm 0.02$	$1.63 \pm 0.03$
7.5	$1.36 \pm 0.03$	$1.46 \pm 0.04$	$1.46 \pm 0.04$	$1.66 \pm 0.05$
10	$1.37 \pm 0.03$	$1.46 \pm 0.04$	$1.46 \pm 0.04$	$1.65 \pm 0.06$

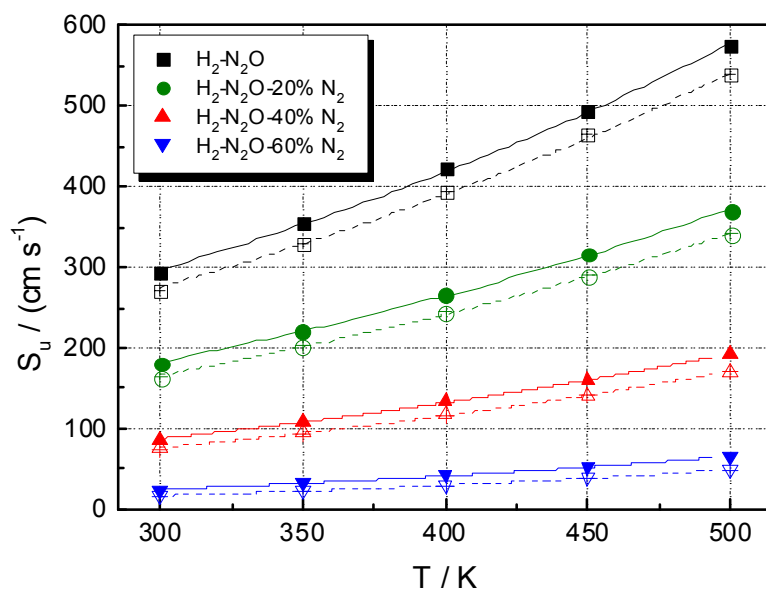


Fig. 1 – Initial temperature influence on laminar burning velocity at various initial pressures: (—)  $p_0 = 1$  bar; (---)  $p_0 = 5$  bar.

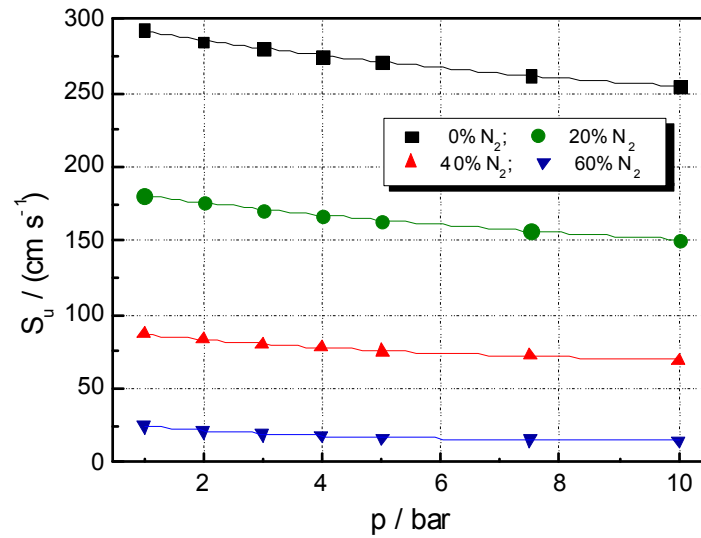
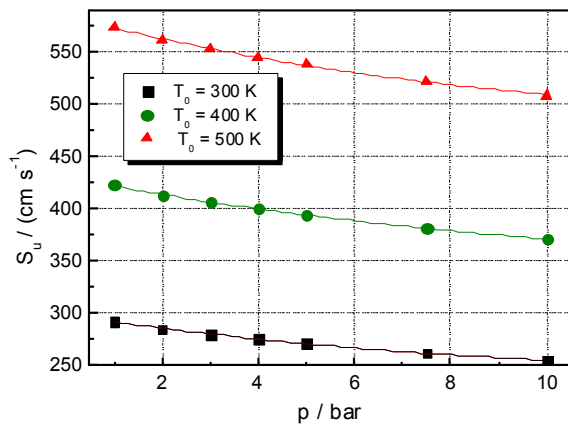
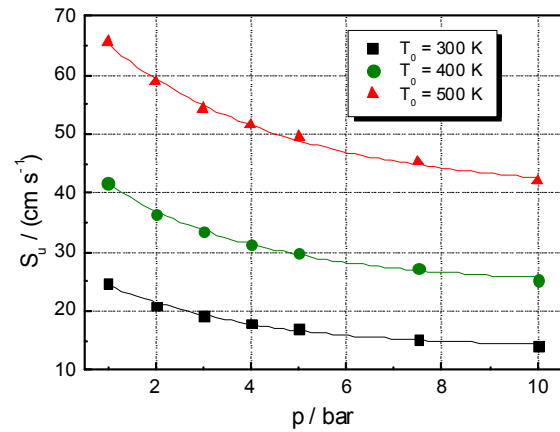


Fig. 2 – Laminar burning velocities of the stoichiometric H<sub>2</sub>-N<sub>2</sub>O mixture diluted with various N<sub>2</sub> amounts, at 300 K and various initial pressures.



(a)

Fig. 3(a) – Laminar burning velocities of the stoichiometric H<sub>2</sub>-N<sub>2</sub>O mixture, at various initial temperatures.



(b)

Fig. 3(b) – Laminar burning velocities of the stoichiometric H<sub>2</sub>-N<sub>2</sub>O-60%N<sub>2</sub> mixture, at various initial temperatures.

Table 2

Baric coefficients,  $-\nu$ , of laminar burning velocities for stoichiometric H<sub>2</sub>-N<sub>2</sub>O mixtures diluted with various N<sub>2</sub> amounts, at various initial temperatures

N <sub>2</sub> /vol% T <sub>0</sub> / K	0	20	40	60
300	0.059 ± 0.006	0.061 ± 0.006	0.114 ± 0.007	0.230 ± 0.002
400	0.055 ± 0.006	0.072 ± 0.008	0.103 ± 0.012	0.215 ± 0.005
500	0.051 ± 0.005	0.067 ± 0.008	0.095 ± 0.012	0.188 ± 0.006

Low absolute values of baric coefficients,  $|\nu| = 0.05\text{--}0.07$  are found for the stoichiometric H<sub>2</sub>-N<sub>2</sub>O and H<sub>2</sub>-N<sub>2</sub>O-20% N<sub>2</sub> mixtures at all temperatures. The increase of N<sub>2</sub> concentration in H<sub>2</sub>-N<sub>2</sub>O-N<sub>2</sub> mixtures up to 60% results in the increase of absolute values of baric coefficients, to

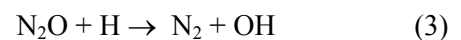
the expected characteristic values for H<sub>2</sub>-air and hydrocarbon-air mixtures. The weak pressure dependence of laminar burning velocities of undiluted stoichiometric H<sub>2</sub>-N<sub>2</sub>O flame at 300 K in the pressure range from 1 to 3 bar is confirmed by data from Bane *et al.*<sup>27</sup> reporting a baric coefficient

$\nu = -0.035$ . Another set of laminar burning velocities, measured at pressures between 10 and 760 mm Hg showed a similar weak dependence on pressure, characterized by a baric coefficient  $\nu = 0.135$ .<sup>16</sup> A similar behavior was already reported for the stoichiometric  $\text{H}_2\text{-O}_2$  mixture diluted with  $\text{N}_2$  (concentrations within 0-30 vol%) where a weak influence of pressure on laminar burning velocities was observed, shown by absolute baric coefficients between 0.1 and 0.05.<sup>33</sup> In nitrogen-diluted  $\text{H}_2\text{-O}_2$  mixtures with  $\text{N}_2$  concentrations higher than 30 vol% (including  $\text{H}_2\text{-air}$ ) slower flames propagate and a stronger pressure influence on  $S_u$  is measured (absolute baric coefficients between 0.1 and 0.3).<sup>33</sup> The data confirmed an earlier suggestion of Lewis and von Elbe<sup>34</sup> who postulated the baric coefficient as a function only of flame velocity, not of the system considered and/or the state of the flammable mixture.

An extended data set of laminar burning velocities, measured for flames stabilized on a Bunsen burner, was reported by Duval and van Tiggelen<sup>19</sup> who examined  $\text{H}_2\text{-N}_2\text{O}$  mixtures with various equivalence ratios, diluted with  $\text{N}_2$ , at ambient initial pressure. A comparison of their results, later used by Coffee<sup>21</sup> for modeling these flames, with a more recent measurement made at 0.8 bar,<sup>25</sup> with the present data from our numerical experiments and from other kinetic modeling study<sup>27</sup> is shown in Fig. 4. A reasonable agreement between measured and computed burning

velocities is found, especially at higher dilutions of flammable  $\text{H}_2\text{-N}_2\text{O}$  mixture, of 30...60 vol%  $\text{N}_2$ . The discrepancy observed between measured and computed laminar burning velocities appears for the non-diluted  $\text{H}_2\text{-N}_2\text{O}$  flame:  $S_{u,\text{exp}}^{19} = 385 \text{ cm s}^{-1}$  versus  $S_{u,\text{calc}} = 295 \text{ cm s}^{-1}$  (present results). It is worth mentioning that the high burning velocity of non-diluted  $\text{H}_2\text{-N}_2\text{O}$  mixture, delivered by experiments at 70 mm Hg 20 and at ambient pressure<sup>19</sup> could be overestimated, since the burning velocities were not stretch-corrected. Later numerical experiments<sup>27</sup> gave a lower value,  $S_u = 329 \text{ cm s}^{-1}$ , in closer agreement with the present computed burning velocities.

A comprehensive set of experimental burning velocities of  $\text{H}_2\text{-N}_2\text{O-60\%Ar}$  mixtures with various equivalence ratios within 0.3 and 1.8, at ambient initial pressure and temperature<sup>23,24</sup> was subject to a detailed modeling using three mechanisms. The sensitivity and reaction pathway analysis performed for each of the three mechanisms demonstrated that the dynamics of the system is determined by a linear reaction chain that governs the energy release rate.<sup>23,24</sup>



and

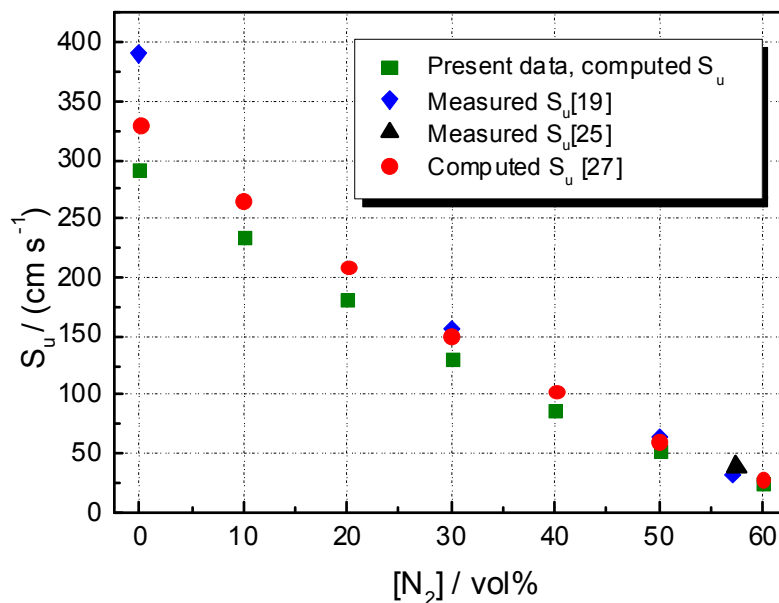
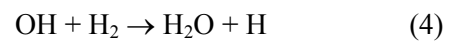
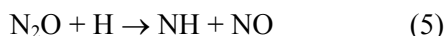
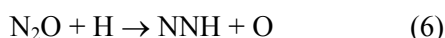


Fig. 4 – Measured and computed laminar burning velocities of stoichiometric  $\text{H}_2\text{-N}_2\text{O}$  mixture diluted with various amounts of  $\text{N}_2$  at 300 K and 1 bar.

A kinetic modeling of flame propagation in  $\text{H}_2\text{-N}_2\text{O-N}_2$  mixtures with various equivalence ratios and various added nitrogen amounts was made by Powell *et al.*<sup>25,26</sup> using a modified Gri-Mech 3.0 mechanism along with two other mechanisms (PPD and “modified” PPD) compiled from recent partial mechanisms for C1-C3 hydrocarbons oxidation<sup>35</sup> and for  $\text{N}_x\text{O}_y/\text{CO}/\text{H}_2/\text{O}_2$  reactions.<sup>22</sup> Their pathway analysis of flame propagation in  $\text{H}_2\text{-N}_2\text{O-N}_2$  mixtures showed that other reactions compete for nitrous oxide conversion:



and



but they contribute only to a small extent of the nitrous oxide conversion. Together with elementary reactions (3) and (4) and with reactions involving  $\text{N}_2\text{H}_x/\text{NH}_x$  species, they account for generation and consumption of H, OH, and O chain carriers.

Based on these findings, we consider important to examine the influence of radical concentrations on the laminar burning velocity, determined by the initial temperature, pressure and  $\text{N}_2$  concentration changes. A set of relevant data concerning the profiles of temperature, of heat release rate and of important radical concentrations in a typical  $\text{H}_2\text{-N}_2\text{O-N}_2$  flame are shown in Fig. 5. The plots are similar for runs at higher initial temperatures and pressures. The mass fractions of H, OH and O increase steadily, following the temperature variation across the flame front. Among them, OH

is present in higher concentrations at all initial conditions.

The influence of initial pressure on H, OH and O peak mass fractions of each flame is shown in Fig. 6, for  $\text{H}_2\text{-N}_2\text{O-N}_2$  systems with variable nitrogen concentration and constant initial temperature. Similar plots were obtained for all studied temperatures, within 300 and 500 K. The increase of nitrogen concentration entails different trends of  $x_H$ ,  $x_{OH}$  and  $x_O$  variation against  $p$ , readily observed for  $\text{H}_2\text{-N}_2\text{O}$  and  $\text{H}_2\text{-N}_2\text{O-20\% N}_2$  systems when compared to systems containing 40 and 60%  $\text{N}_2$ : the flames of these last two mixtures are characterized by a slight pressure influence on radical mass fractions in contrast to the flames of  $\text{H}_2\text{-N}_2\text{O}$  and  $\text{H}_2\text{-N}_2\text{O-20\%N}_2$  systems, characterized by a stronger pressure influence on all radical concentrations. The difference between faster flames (in  $\text{H}_2\text{-N}_2\text{O}$  and  $\text{H}_2\text{-N}_2\text{O-20\% N}_2$  mixtures) and the slower flames (in  $\text{H}_2\text{-N}_2\text{O}$  mixtures diluted with 40 and 60%  $\text{N}_2$ ) appears also in the diagrams plotting the sum of mass fractions for H, O, and OH against pressure [Fig. 6(d)].

It is useful to examine also the pressure influence on the volumetric rate of heat release in  $\text{H}_2\text{-N}_2\text{O-N}_2$  flames, shown in Fig. 7. The pressure influence on the laminar burning velocities (shown in Fig. 1 and 2) and on the volumetric rates of heat release is quite opposite, suggesting the decrease of the laminar burning velocities with pressure cannot be assigned to the thermal factor but to the variation of active species concentrations.

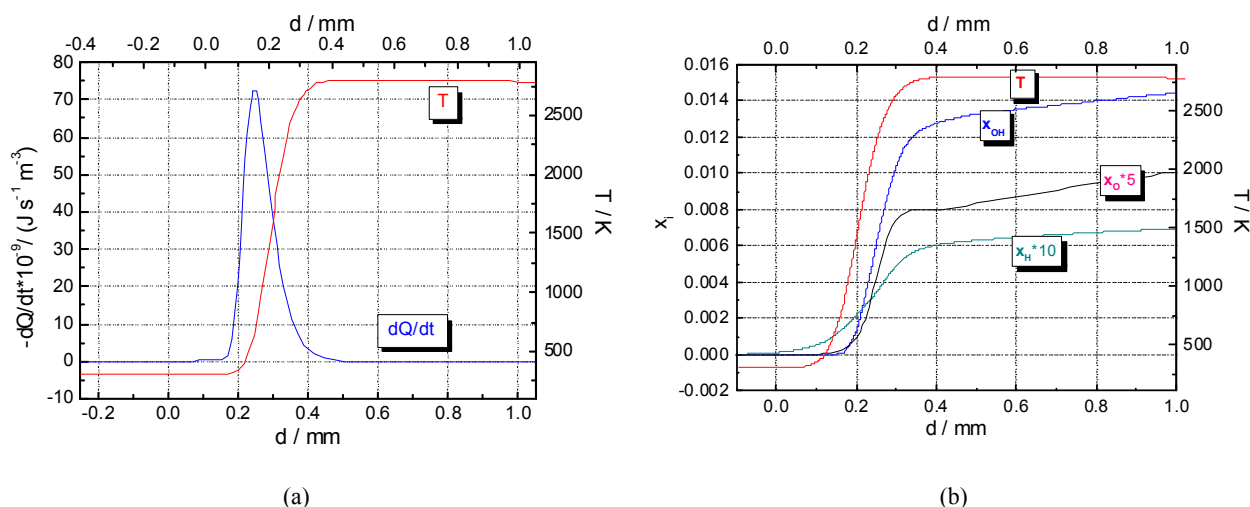


Fig. 5 – Temperature, volumetric rate of heat release (a) and mass fraction profiles of H, OH and O (b) in the flame front of a stoichiometric  $\text{H}_2\text{-N}_2\text{O-20\%N}_2$  mixture at ambient initial conditions.

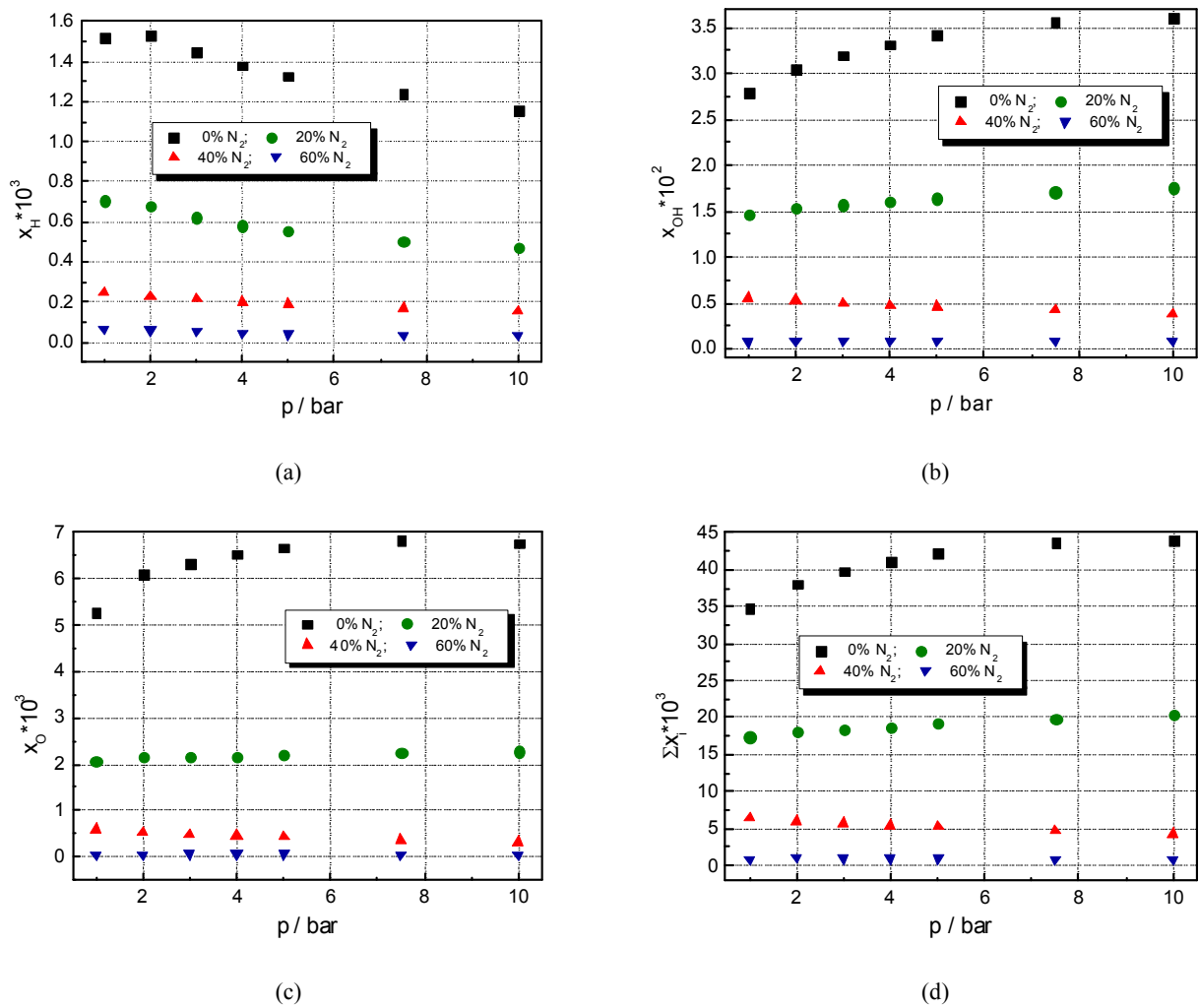


Fig. 6 – Peak mass fractions of H, OH and O ((a)-(c)) and the sum of their peak mass fractions (d) in stoichiometric H<sub>2</sub>-N<sub>2</sub>O-N<sub>2</sub> flames with various N<sub>2</sub> concentrations as functions of the total initial pressure at  $T_0 = ct = 300$  K.

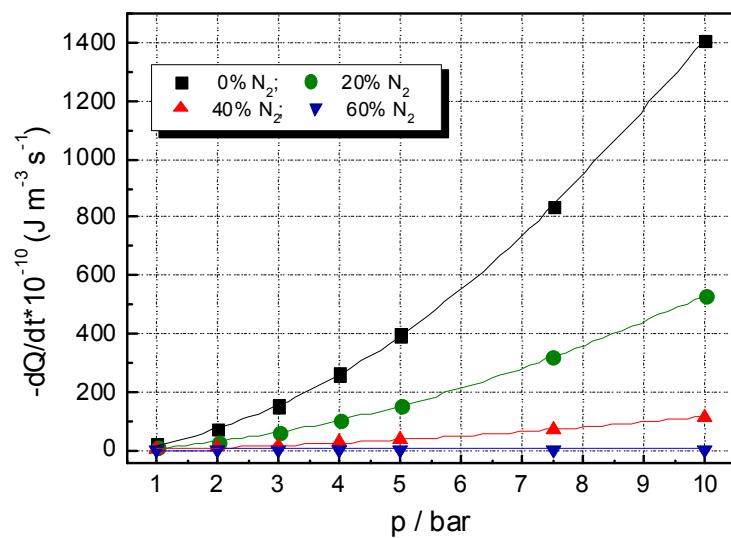


Fig. 7 – Volumetric rate of heat release in H<sub>2</sub>-N<sub>2</sub>O-N<sub>2</sub> flames with various N<sub>2</sub> concentrations as functions of the total initial pressure;  $T_0 = 300$  K.

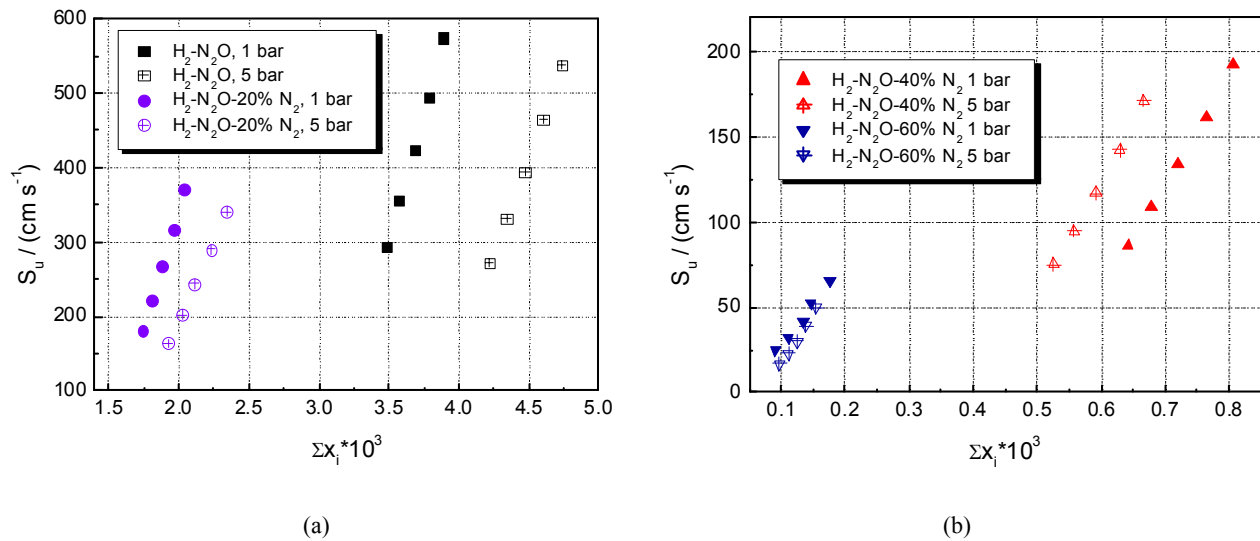


Fig. 8 – Laminar burning velocities of stoichiometric  $\text{H}_2\text{-N}_2\text{O-N}_2$  mixtures *versus* the sum of peak mass fractions of H, O and OH: (a)  $\text{H}_2\text{-N}_2\text{O}$  and  $\text{H}_2\text{-N}_2\text{O-20\%N}_2$  mixtures; (b)  $\text{H}_2\text{-N}_2\text{O-N}_2$  mixtures containing 40 and 60%  $\text{N}_2$ . Each data set corresponds to various initial temperatures (300...500 K).

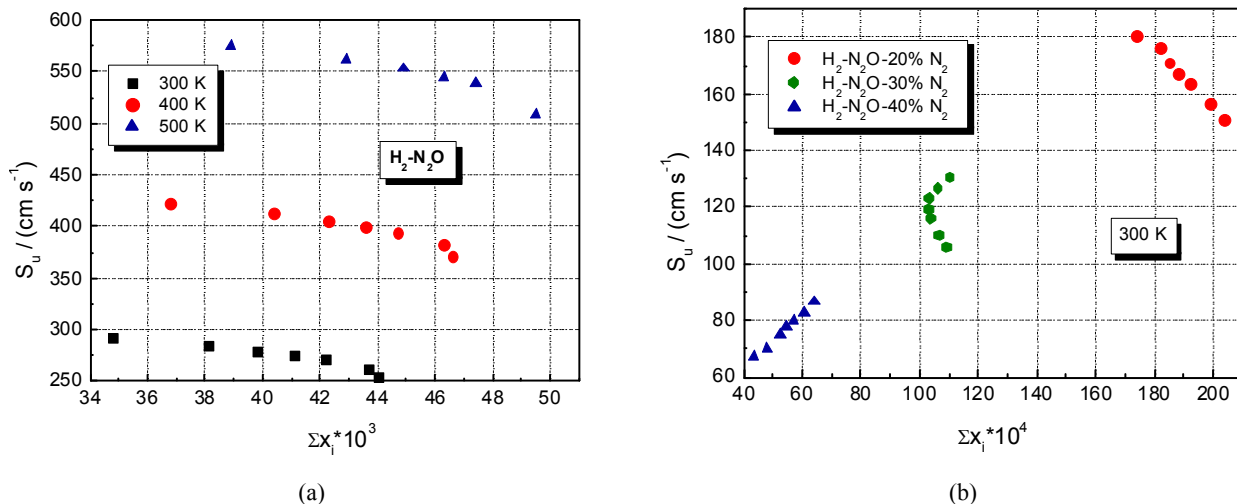


Fig. 9 – Laminar burning velocities versus the sum of peak mass fractions of H, O and OH; data computed at several initial temperatures; each data set corresponds to various initial pressures (1...10 bar): (a)  $\text{H}_2\text{-N}_2\text{O}$  mixture; (b)  $\text{H}_2\text{-N}_2\text{O-N}_2$  mixtures at 300 K.

For  $\text{H}_2\text{-O}_2$ -diluent flames Warnatz found a good correlation between  $S_u$  and the peak concentrations of H in the reaction zone.<sup>36,37</sup> Similar correlations between the laminar burning velocity and the maximum radical concentrations of H and OH radicals were found in premixed flames of  $\text{H}_2$ ,  $\text{CH}_4$  and  $\text{C}_2\text{H}_4$  with air.<sup>38</sup> In the case of  $\text{H}_2\text{-N}_2\text{O-N}_2$  flames it is necessary to take also into account the O atoms, generated by  $\text{N}_2\text{O}$  dissociation in the flame, which are present in significant amounts. Therefore, it seems important to examine a possible correlation between the laminar burning velocity and the sum of the mass fractions of active radical species H, O and OH.

Plots of  $S_u$  *versus*  $\Sigma x_i$  are shown in Fig. 8 for  $\text{H}_2\text{-N}_2\text{O-N}_2$  mixtures, at various compositions and initial pressures. At all examined pressures the laminar burning velocities increase with the total maximum radical concentration  $\Sigma x_i$ , for these data sets that contain  $S_u$  and  $\Sigma x_i$  determined at various initial temperatures. These diagrams confirm the observed increase of laminar burning velocities with temperature.

Similar plots of  $S_u$  *versus*  $\Sigma x_i$  for  $\text{H}_2\text{-N}_2\text{O}$  diluted with  $\text{N}_2$  of various concentrations, at  $T_0 = \text{ct} = 300$  K, are shown in Fig. 9. For these

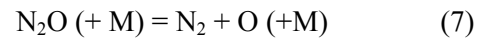


data sets, plotting  $S_u$  against  $\Sigma x_i$  determined at various initial pressures, the trend is different, as influenced by the amount of added nitrogen. For faster burning mixtures ( $H_2-N_2O$  and  $H_2-N_2O-20\%N_2$ ) one can observe the decrease of laminar burning velocities when the total amount of radicals increases. It suggests that the decrease of laminar burning velocity with the increase of initial pressure can be understood by the suppression of overall chemical reaction due to the decrease of H and OH mole fractions in flames. For each examined flame, the balance between the rates of H, O and OH generation and consumption at various pressures results in the change of the overall reaction rate, which has a most important influence on the laminar burning velocity.

In contrast to them, in the slower burning mixtures ( $H_2-N_2O$  diluted with 40% and 60%  $N_2$ ) the increase of total amount of radicals is accompanied by the increase of laminar burning velocities, since both  $S_u$  and  $\Sigma x_i$  decrease when pressure changes from 1 to 10 bar. The difference of behavior is better shown in Fig. 9(b), where data referring to  $H_2-N_2O$  flames diluted with 20, 30 and 40%  $N_2$  were plotted. The opposite variation of  $S_u$  vs.  $\Sigma x_i$  is seen for  $H_2-N_2O$  flames diluted with 20 and 40%  $N_2$ . Between them, the plot of  $H_2-N_2O-30\%N_2$  flames shows a complex, mixed influence of pressure: at pressures between 1 and 4 bar, both  $S_u$  and  $\Sigma x_i$  decrease, at pressures between 5 and 10 bar the laminar burning velocity decreases with pressure whereas  $\Sigma x_i$  increases.

The differences between  $H_2-N_2O$  flames diluted by 20, 30 and 40 vol%  $N_2$  could be partly explained by the results of sensitivity analyses performed under present modeling experiments.

Our sensitivity analysis with respect to the laminar burning velocities of  $N_2$ -diluted  $H_2-N_2O$  flames, computed with GRI-Mech 3.0 mechanism, outlined the reactions with the highest influence on flame propagation, besides reaction (3):



and



In Fig. 10 the sensitivity coefficients of four important reactions (3, 7, 8 and 9) are plotted. The results confirm the fact that reaction (3) ( $N_2O + H = N_2 + OH$ ) is the most important for the temperature increase as it is highly exothermic. Since reaction (3) forms OH radicals that further react with  $H_2$  to produce  $H_2O$ , it is responsible for an additional heat release.

The difference between the  $H_2-N_2O$  flames diluted by 20, 30 and 40 vol%  $N_2$  is given by a positive sensitivity coefficient in respect to reaction (8) for the flame diluted with 20%  $N_2$ , whereas negative sensitivity coefficients in respect to this reaction are found for  $H_2-N_2O$  flames diluted with 30 and 40 vol%  $N_2$ . The examined reaction (8), responsible for O consumption and OH generation (together with reaction 3) could thus influence the overall chemical reaction and further on, the laminar burning velocity.

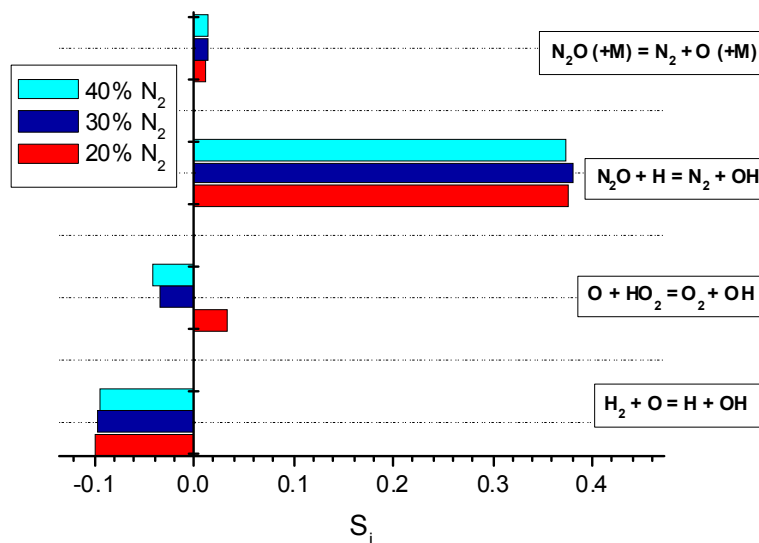


Fig. 10 – Sensitivity coefficients of laminar burning velocities in respect to rate constants of several reactions, for  $N_2$ -diluted  $H_2-N_2O$  stoichiometric flames propagating at ambient initial conditions.

These results show that the detailed chemical modeling is a valuable tool for characterizing flammable gaseous mixtures, difficult to study experimentally under wide ranges of initial composition, pressure and temperature. Such a case is the H<sub>2</sub>-N<sub>2</sub>O mixture, prone to sustain fast-propagating deflagrations especially at the stoichiometric ratio of 1:1, due to high exothermal effect of their reaction. Nitrogen addition to H<sub>2</sub>-N<sub>2</sub>O results in milder explosions, of similar characteristics with flammable fuel-air gaseous mixtures.

The computed laminar burning velocities are of fundamental importance for describing the laminar and turbulent flame propagation, together with the measured profiles of temperature, species concentrations and rate of heat delivery across the flame. At the same time, the laminar burning velocities are useful input parameters for CFD (Computational Fluid Dynamics) simulations of deflagrations in confined spaces or of vented explosions.

## CONCLUSIONS

The explosion propagation in flammable gaseous mixtures can be well characterized by the adiabatic laminar burning velocities, without interference of turbulence, heat transfer to an enclosure or other perturbations.

The present study reports the laminar burning velocities of H<sub>2</sub>-N<sub>2</sub>O and H<sub>2</sub>-N<sub>2</sub>O-N<sub>2</sub> mixtures, obtained by the chemical modeling of their combustion, using the GRI-Mech 3.0 mechanism.

Examination of the laminar burning velocities as functions of pressure (at constant T<sub>0</sub>) or temperature (at constant p<sub>0</sub>) for the stoichiometric H<sub>2</sub>-N<sub>2</sub>O and H<sub>2</sub>-N<sub>2</sub>O-N<sub>2</sub> mixtures (N<sub>2</sub> = 10...60 vol%) was made by means of empirical power laws, which delivered the baric and thermal coefficients of the laminar burning velocities. Their values are influenced mostly by the initial composition of these mixtures.

The structure of stoichiometric H<sub>2</sub>-N<sub>2</sub>O and H<sub>2</sub>-N<sub>2</sub>O-N<sub>2</sub> flames was characterized by the temperature, volumetric rate of heat release and concentration profiles of chemical species within the flame front. Each property was examined as a function of the initial conditions (composition, pressure, temperature) of flammable mixtures.

In all mixtures, the laminar burning velocities were examined in connection with the total

amount of free radicals, revealing opposite behaviors of fast burning mixtures (H<sub>2</sub>-N<sub>2</sub>O and H<sub>2</sub>-N<sub>2</sub>O-20% N<sub>2</sub>) and slow burning mixtures (H<sub>2</sub>-N<sub>2</sub>O flames diluted with 40% and 60% N<sub>2</sub>) when the pressure influence is discussed. For each examined flame, the balance between the rates of H, O and OH generation and consumption at various pressures determines changes of the overall reaction rate, which has a most important influence on laminar burning velocity.

*Acknowledgements.* The present study was partially financed by the Roumanian Academy under research project "Dynamics of fast oxidation and decomposition reactions in homogeneous systems" of "Ilie Murgulescu" Institute of Physical Chemistry-Bucharest.

## REFERENCES

1. T. Hirano, *J. Loss Prev. Process. Ind.*, **2004**, *17*, 29–34.
2. L. Vandebroek, F. Van den Schoor, F. Verplaetsen, J. Berghmans, H. Winter and E. van't Oost, *J. Hazard. Mater.*, **2005**, *120*, 57–65.
3. C. Merrill, "Nitrous Oxide Explosive Hazards", Defense Explosives Safety Seminar, Palm Springs, CA, 2008, p. 38.
4. F. Scott, R. Van Dolah and M. Zabetakis, *Proc. Combust. Inst.*, **1957**, *6*, 540–545.
5. U. Pfahl, M. Ross, and J. Shepherd, *Combust. Flame*, **2000**, *123*, 140–158.
6. F. Kollmer and W. Hölderich, *Chemie Ing. Techn.*, **2003**, *75*, 912–914.
7. V.V. Zamaschikov, V.A. Bunev, K.A. Dubkov, G.I. Panov and V.S. Babkin, *Proc. Int. Seminar on Flame Structure*, Novosibirsk, Russia, **2005**.
8. T. Meye, E. Brandes, M. Höding and S. Busse, *Proc. 9th ISPHMIE*, Cracow, Poland, **2012**.
9. S. Coronel, R. Mével, S. Bane and J. Shepherd, *Proc. Combust. Inst.*, **2013**, *34*, 895–902.
10. Y. Koshihara, T. Takigawa, Y. Matsuoka and H. Ohtani, H., *J. Hazard. Mater.*, **2010**, *183*, 746–753.
11. Y. Koshihara, T. Nishida, N. Morita and H. Ohtani, *Process Saf. Environ. Prot.*, **2015**, *98*, 11–15.
12. D. Razus, M. Mitu, V. Giurcan, and D. Oancea, *J Loss Prev. Process Ind.*, **2017**, *49*, 418–426.
13. L. Q. Wang, H. H. Ma and Z. W. Shen, *Fuel*, **2020**, *260*, 116355.
14. Z. Liang, J. Karnesky and J. Shepherd, *Graduate Aeronaut. Lab., California Inst. Technol., Tech. Report No. FM2006-003*, **2006**.
15. B. Zhang, H. D. Ng, R. Mével and J. H. Lee, *Int. J. Hydrogen Energy*, **2011**, *36*, 5707–5716.
16. W. Parker and H. G. Wolfhard. *Proc. 4<sup>th</sup> Symp.(Intern.) on Combustion*, **1953**, *4*, 420–428.
17. G. Dixon-Lewis, M. Sutton and A. Williams, *Combust. Flame*, **1964**, *8*, 85–87.
18. P. Gray, R. Mackinven and D. B. Smith, *Combust. Flame*, **1967**, *11*, 217–226.
19. A. Duval and P. J. Van Tiggelen, *Bull. Acad. Roy. Belges*, **1967**, *53*, 366–402.

20. P. Gray, S. Holland and D. B. Smith, *Combust. Flame*, **1970**, *14*, 361–374.
21. T. P. Coffee, *Combust. Flame*, **1986**, *65*, 53–60.
22. M. T. Allen, R. A. Yetter and F. L. Dryer, *Combust. Flame*, **1998**, *112*, 302–311.
23. R. Mével, F. Lafosse, N. Chaumeix, G. Dupré and C.E. Paillard, *Proc. 4<sup>th</sup> European Combust. Meeting Wien*, **2009**.
24. R. Mével, F. Lafosse, N. Chaumeix, G. Dupré and C.-E. Paillard, *Int. J. Hydrogen Energy*, **2009**, *34*, 9007–9018.
25. O. A. Powell, P. Papas and C. Dreyer, *Combust. Sci. Technol.*, **2009**, *181*, 917–936.
26. O. A. Powell, P. Papas and C. Dreyer, *Combust. Sci. Technol.*, **2010**, *182*, 252–283.
27. S. P. M. Bane, R. Mével, S. A. Coronel and J. E. Shepherd, *Int. J. Hydrogen Energy*, **2011**, *36*, 10107–10117.
28. R. C. Sausa, W. R. Anderson, D. C. Dayton, C. M. Faust and S. L. Howard, *Combust. Flame*, **1993**, *94*, 407–425.
29. M. Brown and D. Smith, *Proc. Combust. Inst.*, **1994**, *25*, 1011–1018.
30. R. C. Sausa and D. T. Venizelos, *Proc. Optical Diagnostics for Fluids, Solids, and Combustion*, San Diego, USA, Vol 4448, **2001**.  
<https://doi.org/10.1117/12.449360>.
31. C. K. Law, “Combustion Physics”, Cambridge University Press, New York, 2006.
32. COSILAB Version 3.0.3, Rotexo-Softpredict-Cosilab GmbH & Co KG: Bad Zwischenhahn, 2012.  
<https://www.rotexo.com/index.php/en/>
33. D. Razus, M. Mitu, V. Giurcan, C. Movileanu and D. Oancea, *Rev. Roum. Chim*, **2020**, *65*, 529–537.
34. B. Lewis and G. von Elbe, “Combustion, Explosion and Flames of Gases”, Academic Press, 3<sup>rd</sup> Ed., New York and London, 1987.
35. X. Qin, H. Kobayashi and T. Niioka, *Exp. Thermal Fluid Sci.*, **2000**, *21*, 58–63.
36. J. Warnatz, *Combust. Sci. Technol.*, **1981**, *26*, 203–213.
37. F. Behrendt and J. Warnatz, *Int. J. Hydrogen Energy*, **1985**, *10*, 749–702.
38. E. Hu, Z. Huang, J. He and H. Miao, *Int. J. Hydrogen Energy*, **2009**, *34*, 8741–8755.

